Joint Exploitation of TDOA and PCL Techniques for 2D Target Localization

Augusto Aubry, *Senior Member, IEEE*, Vincenzo Carotenuto, *Senior Member, IEEE*, Antonio De Maio, *Fellow, IEEE*, and Luca Pallotta, *Senior Member, IEEE*

***Abstract*—This paper is focused on non-cooperative target position estimation via the joint use of Two-Dimensional (2D) hyperbolic and elliptic passive location techniques based on Time Difference Of Arrival (TDOA) and Passive Coherent Locator (PCL) measurements, respectively. A fusion strategy is laid down at the signal processing level to obtain a reliable estimate of the current target position. With reference to the scenario with a single transmitter of opportunity, the mathematical model for joint exploitation of TDOA and PCL strategies is formulated. Then, the Cramer Rao Lower Bound (CRLB) for the cartesian coordinates of the target is established and the theoretical performance gains achievable over the localization technique using only TDOA or PCL observations are assessed. Finally, TDOA-PCL hybrid 2D localization algorithms are provided and their performance in terms of Root Mean Square Error (RMSE) is compared with the square root of the CRLB.**

Keywords*—*Time Difference of Arrivals, Passive Coherent Location, Target Localization, Information Fusion, Sensor Fusion.

I. Introduction

A big challenge in modern localization systems is the possibility to estimate the position of a non-cooperative target via passive techniques [1]–[10]. These approaches are of great strategic interest being able to operate without the availability of a dedicated transmitter which is indeed mandatory in active localization systems. The remarkable consequence is a significant reduction of the system cost as well as the possibility to localize a target without being localized.

Due to the importance of the problem, numerous solutions have been proposed in open literature mostly relying on hyperbolic and elliptic positioning [11]–[16]. The former class is based on Time Difference Of Arrival (TDOA) measurements from signals transmitted by the target of interest (radar or communication waveforms depending on the target's mission) and collected at the receiving nodes. The latter, usually referred to in radar literature as a Passive Coherent Locator (PCL), can be accomplished using bistatic target range measurements obtained via signals transmitted by one/multiple illuminators of opportunity [17, Chap. 11], reflected by the target, and acquired by the passive receiver/receivers. Basically, each measurement localizes the target over an ellipsoid and the intersection of multiple ellipsoids due to different transmitter-receiver pairs enables target positioning. In this respect different transmitters of opportunity could be considered such as frequency modulated radio [18], [19], digital audio broadcast and digital video broadcast terrestrial [20]. Many prototypes, possibly exploiting multiple transmitters [19], have been developed over the years [21] and their performance has been assessed [22], [23] with reference to a multitude of applications ranging form Air Traffic Control (ATC) to indoor surveillance [24]–[26].

In open literature several algorithms have been proposed to estimate the cartesian coordinates of the target with reference to TDOA or elliptic (in particular PCL) localization approaches. Some examples are represented by the Least Squares (LS) [27], the Constrained Least Squares (CLS) [11], [27], the Two-Step Estimation (TSE) [28], and the Iterative Constrained Least Squares (ICLS) algorithms. Furthermore, to capitalize the benefits of the possible availability of TDOA and PCL measurements, some fusion algorithms have been developed to improve the estimation accuracy achieved using only one of the aforementioned approaches [29].

However, it is worth pointing out that previous strategies have been mainly focused on the independent operation of each sub-system up to bistatic tracking of targets [29]; fusion is then performed at the data processing level. In this respect the present study is settled up before the tracking process, i.e. when the measurements of TDOA and PCL are jointly used to obtain an estimate of the target position which could be then used for track update. Otherwise stated, fusion is performed at signal processing level. Other studies on TDOA and PCL fusion can be found in [30] and [31].

The paper is organized as follows. With reference to a two-dimensional (2D) scenario[1] with a single transmitter of opportunity, in Section II, the mathematical model for the joint exploitation of TDOA and PCL observations is developed. In Section III, the Cramer Rao Lower Bound (CRLB) for the cartesian coordinates of the target is established and the performance gains achievable over localization techniques using only TDOA or PCL is assessed. In addition, a discussion on the identifiability of the studied localization problem is carried on. In Section IV, TDOA-PCL hybrid localization algorithms are provided to estimate target position, whereas, in Section V, their performance is assessed resorting to Monte-Carlo simulations and considering as figure of merit the position Root Mean Square Error (RMSE). Finally, in Section VI conclusions

Augusto Aubry and Antonio De Maio are with Università degli Studi di Napoli "Federico II", DIETI, Via Claudio 21, I-80125 Napoli, Italy. E-mail: augusto.aubry@unina.it, ademaio@unina.it.

Vincenzo Carotenuto and Luca Pallotta are with CNIT udr Università "Federico II", via Claudio 21, I-80125 Napoli, Italy. E-mail: vincenzo.carotenuto@unina.it, luca.pallotta@unina.it.

[1]Note that, it is straightforward to generalize the developed approach to a three-dimensional (3D) scenario.

are drawn and some future research is discussed.

NOTATION

We adopt the notation of using boldface for vectors $\boldsymbol{a}$ (lower case), and matrices $\boldsymbol{A}$ (upper case). The n-th element of $\boldsymbol{a}$ and the (n,m)-th entry of $\boldsymbol{A}$ are denoted by a_n and $\boldsymbol{A}_{n,m}$, respectively. The transpose operator is represented by the symbol $(\cdot)^T$. $\boldsymbol{I}$ and $\boldsymbol{0}$ indicate respectively the identity matrix and the matrix with zero entries (their size is determined from the context). The trace operator is denoted by $\mathrm{Tr}(\cdot)$ and $\|\cdot\|$ indicates the Euclidean vector norm. $\mathbb{E}[\cdot]$ stands for statistical expectation whereas $\mathbb{R}^N$ and $\mathbb{R}^{N\times M}$ are the sets of N-dimensional vectors of real numbers and of $N\times M$ real matrices, respectively. $\mathbf{diag}\,(\boldsymbol{a})$ indicates the diagonal matrix whose i-th diagonal element is the i-th entry of $\boldsymbol{a}$. Finally, the curled inequality symbol $\succeq$ is used to denote generalized matrix inequality: for any $\boldsymbol{A}\in\mathbb{R}^{N\times N}$, $\boldsymbol{A}\succeq\boldsymbol{0}$ means that $\boldsymbol{A}$ is a positive semi-definite matrix.

II. PROBLEM FORMULATION AND SYSTEM MODEL

Let us consider a passive location system composed of N sensor nodes each equipped with both a Time Of Arrival (TOA) and a PCL receiver. Let

- $\boldsymbol{s}_i=[x_i,y_i]^T\in\mathbb{R}^2$, $i=1,\ldots,N$, the sensor nodes positions;
- $\boldsymbol{u}=[x_e,y_e]^T\in\mathbb{R}^2$ the target position;
- $\boldsymbol{t}=[x_t,y_t]^T\in\mathbb{R}^2$ the transmitter of opportunity position.

The vectors $\boldsymbol{s}_i$ and $\boldsymbol{t}$ are supposed perfectly known and the TDOA measurements are computed with respect to a specific sensor which, without loss of generality, is $\boldsymbol{s}_1$. Using the above definitions, in the next 3 sub-sections the observation models for TDOA, PCL, and hybrid TDOA/PCL are laid down.

A. TDOA System Model

Consider sensor 1 as reference node and denote by τ_i the TOA of the signal emitted by the target and received at the i-th sensor node. TDOA measurements can be expressed as

$$\tau_{i1}=\tau_i-\tau_1,\quad i=2,\ldots,N. \tag{1}$$

If c is the speed of light in the vacuum, equation (1) can be rewritten in terms of range-difference measurements as

$$r_{i1}=c\tau_{i1}=c\tau_i-c\tau_1=r_i-r_1=\|\boldsymbol{s}_i-\boldsymbol{u}\|-\|\boldsymbol{s}_1-\boldsymbol{u}\|,\quad i=2,\ldots,N. \tag{2}$$

Solving for $\|\boldsymbol{s}_i-\boldsymbol{u}\|$ and squaring both sides of (2), after some algebraic manipulation, yields

$$\left(\boldsymbol{s}_i^T-\boldsymbol{s}_1^T\right)\boldsymbol{u}+r_{i1}r_1=\frac{1}{2}\left(\|\boldsymbol{s}_i\|^2-\|\boldsymbol{s}_1\|^2-r_{i1}^2\right). \tag{3}$$

Now, considering the noisy range-difference measurements

$$\tilde{r}_{i1}=(r_i+n_{\mathrm{TDOA},i})-(r_1+n_{\mathrm{TDOA},1})=r_{i1}+\delta_{\mathrm{TDOA},i},\quad i=2,\ldots,N, \tag{4}$$

where $\delta_{\mathrm{TDOA},i}=(n_{\mathrm{TDOA},i}-n_{\mathrm{TDOA},1})$, $i=2,\ldots,N$, with $n_{\mathrm{TDOA},i}$, $i=1,\ldots,N$, independent and identically distributed (i.i.d.) zero-mean Gaussian random variables with variance σ^2_{TDOA}, the true range-difference measurements can be expressed as

$$r_{i1}=\tilde{r}_{i1}-\delta_{\mathrm{TDOA},i},\quad i=2,\ldots,N. \tag{5}$$

Substituting (5) in (3) and ignoring the term $\delta^2_{\mathrm{TDOA},i}$ leads to

$$\frac{1}{2}\left(\tilde{r}_{i1}^2-\|\boldsymbol{s}_i\|^2+\|\boldsymbol{s}_1\|^2\right)+\left[\left(\boldsymbol{s}_i^T-\boldsymbol{s}_1^T\right),\ \tilde{r}_{i1}\right]\begin{bmatrix}\boldsymbol{u}\\ r_1\end{bmatrix}=(\tilde{r}_{i1}+r_1)\,\delta_{\mathrm{TDOA},i},\quad i=2,\ldots,N, \tag{6}$$

which can be cast in compact form as

$$\boldsymbol{a}_{\mathrm{TDOA}}-\boldsymbol{H}_{\mathrm{TDOA}}\boldsymbol{\theta}=\boldsymbol{B}_{\mathrm{TDOA}}\boldsymbol{\delta}_{\mathrm{TDOA}}, \tag{7}$$

where $\boldsymbol{\theta}=[\boldsymbol{u}^T,r_1]^T$ and

$$\boldsymbol{a}_{\mathrm{TDOA}}=\frac{1}{2}\begin{bmatrix}\tilde{r}_{21}^2-\|\boldsymbol{s}_2\|^2+\|\boldsymbol{s}_1\|^2\\ \tilde{r}_{31}^2-\|\boldsymbol{s}_3\|^2+\|\boldsymbol{s}_1\|^2\\ \vdots\\ \tilde{r}_{N1}^2-\|\boldsymbol{s}_N\|^2+\|\boldsymbol{s}_1\|^2\end{bmatrix} \tag{8}$$

$$\boldsymbol{H}_{\mathrm{TDOA}}=-\begin{bmatrix}\left(\boldsymbol{s}_2^T-\boldsymbol{s}_1^T\right) & \tilde{r}_{21}\\ \left(\boldsymbol{s}_3^T-\boldsymbol{s}_1^T\right) & \tilde{r}_{31}\\ \vdots & \vdots\\ \left(\boldsymbol{s}_N^T-\boldsymbol{s}_1^T\right) & \tilde{r}_{N1}\end{bmatrix} \tag{9}$$

$$\boldsymbol{\delta}_{\mathrm{TDOA}}=\begin{bmatrix}\delta_{\mathrm{TDOA},2}\\ \delta_{\mathrm{TDOA},3}\\ \vdots\\ \delta_{\mathrm{TDOA},N}\end{bmatrix} \tag{10}$$

$$\boldsymbol{B}_{\mathrm{TDOA}}=\mathbf{diag}\left([\tilde{r}_{21}+r_1,\tilde{r}_{31}+r_1,\ldots,\tilde{r}_{N1}+r_1]\right). \tag{11}$$

Finally, $\boldsymbol{\delta}_{\mathrm{TDOA}}\in\mathbb{R}^{(N-1)\times 1}$ is a zero-mean Gaussian vector with covariance matrix

$$\boldsymbol{Q}_{\mathrm{TDOA}}=\mathbb{E}\left[\boldsymbol{\delta}_{\mathrm{TDOA}}\boldsymbol{\delta}_{\mathrm{TDOA}}^T\right]=\sigma^2_{\mathrm{TDOA}}\left[\boldsymbol{I}_{N-1}+\boldsymbol{1}_{N-1}\boldsymbol{1}_{N-1}^T\right]. \tag{12}$$

B. PCL System Model

Unlike TDOA, a conventional PCL system does not require a reference sensor and, after classic PCL cross-correlation based processing, the following N bistatic delay/range measurements are available

$$r_{ti}=c\tau_{ti}=\|\boldsymbol{t}-\boldsymbol{u}\|+\|\boldsymbol{s}_i-\boldsymbol{u}\|-L_i,\quad i=1,\ldots,N, \tag{13}$$

where $L_i = \|\boldsymbol{s}_i - \boldsymbol{t}\|$. Let us recast the previous equation into an equivalent rather convenient representation for the development of position estimation algorithms. Specifically, starting from the bistatic ranges r_{ti}, let us define the following range-differences

$$r_{ti1} = r_{ti} - r_{t1} = \|\boldsymbol{s}_i - \boldsymbol{u}\| - \|\boldsymbol{s}_1 - \boldsymbol{u}\| - L_{i1}, \quad i = 2, \ldots, N, \tag{14}$$

where $L_{i1} = L_i - L_1$, which can be rearranged as

$$\|\boldsymbol{s}_i - \boldsymbol{u}\| = r_{ti1} + L_{i1} + \|\boldsymbol{s}_1 - \boldsymbol{u}\|, \quad i = 2, \ldots, N. \tag{15}$$

Squaring both sides of (15), after some algebraic manipulation, yields

$$\begin{aligned} &2\left(\boldsymbol{s}_i^T - \boldsymbol{s}_1^T\right)\boldsymbol{u} + 2\left(r_{ti1} + L_{i1}\right) r_1 \\ &\quad = \|\boldsymbol{s}_i\|^2 - \|\boldsymbol{s}_1\|^2 - \left(r_{ti1} + L_{i1}\right)^2, \quad i = 2, \ldots, N. \end{aligned} \tag{16}$$

Now, considering the noisy bistatic range-difference measurements

$$\begin{aligned} \tilde{r}_{ti1} &= \left(r_{ti} + n_{\text{PCL},i}\right) - \left(r_{t1} + n_{\text{PCL},1}\right) \\ &= r_{ti1} + \delta_{\text{PCL},i}, \quad i = 2, \ldots, N, \end{aligned} \tag{17}$$

where $\delta_{\text{PCL},i} = (n_{\text{PCL},i} - n_{\text{PCL},1})$, $i = 2, \ldots, N$, and $n_{\text{PCL},i}$, $i = 1, \ldots, N$, i.i.d. zero-mean Gaussian random variables with variance σ^2_{PCL}, the true bistatic range-difference measurements can be expressed as

$$r_{ti1} = \tilde{r}_{ti1} - \delta_{\text{PCL},i}, \quad i = 2, \ldots, N. \tag{18}$$

Substituting (18) in (16) and ignoring the $\delta^2_{\text{PCL},i}$ term leads to

$$\begin{aligned} &\frac{1}{2}\left[\left(\tilde{r}_{ti1} + L_{i1}\right)^2 - \|\boldsymbol{s}_i\|^2 + \|\boldsymbol{s}_1\|^2\right] \\ &\quad + \left[\left(\boldsymbol{s}_i^T - \boldsymbol{s}_1^T\right) \ \left(\tilde{r}_{ti1} + L_{i1}\right)\right]\begin{bmatrix}\boldsymbol{u} \\ r_1\end{bmatrix} \\ &\quad = \left[\left(\tilde{r}_{ti1} + L_{i1}\right) + r_1\right]\delta_{\text{PCL},i}, \quad i = 2, \ldots, N. \end{aligned} \tag{19}$$

As to the sensor 1

$$r_{t1} = \|\boldsymbol{t} - \boldsymbol{u}\| + \|\boldsymbol{s}_1 - \boldsymbol{u}\| - L_1, \tag{20}$$

which can be rearranged as

$$\|\boldsymbol{t} - \boldsymbol{u}\| = r_{t1} + L_1 - \|\boldsymbol{s}_1 - \boldsymbol{u}\|. \tag{21}$$

Squaring both sides of (21), after some algebraic manipulation, yields

$$2\left(\boldsymbol{s}_1^T - \boldsymbol{t}^T\right)\boldsymbol{u} + 2\left(r_{t1} + L_1\right) r_1 = \left(r_{t1} + L_{i1}\right)^2 + \|\boldsymbol{s}_1\|^2 - \|\boldsymbol{t}\|^2. \tag{22}$$

Again, since

$$r_{t1} = \tilde{r}_{t1} - n_{\text{PCL},1}, \tag{23}$$

ignoring the $n^2_{\text{PCL},1}$ term, it follows that

$$\begin{aligned} &\frac{1}{2}\left[\left(\tilde{r}_{t1} + L_1\right)^2 + \|\boldsymbol{s}_1\|^2 - \|\boldsymbol{t}\|^2\right] \\ &\quad + \left[\left(\boldsymbol{t}^T - \boldsymbol{s}_1^T\right), \ -\left(\tilde{r}_{t1} + L_1\right)\right]\begin{bmatrix}\boldsymbol{u} \\ r_1\end{bmatrix} \\ &\quad = \left[\left(\tilde{r}_{t1} + L_1\right) - r_1\right] n_{\text{PCL},1}. \end{aligned} \tag{24}$$

The previous equations can be expressed in a compact matrix form as

$$\boldsymbol{a}_{\text{PCL}} - \boldsymbol{H}_{\text{PCL}}\boldsymbol{\theta} = \boldsymbol{B}_{\text{PCL}}\boldsymbol{\delta}_{\text{PCL}}, \tag{25}$$

where

$$\boldsymbol{a}_{\text{PCL}} = \frac{1}{2}\begin{bmatrix} \left(\tilde{r}_{t1} + L_1\right)^2 + \|\boldsymbol{s}_1\|^2 - \|\boldsymbol{t}\|^2 \\ \left(\tilde{r}_{t21} + L_{21}\right)^2 - \|\boldsymbol{s}_2\|^2 + \|\boldsymbol{s}_1\|^2 \\ \left(\tilde{r}_{t31} + L_{31}\right)^2 - \|\boldsymbol{s}_3\|^2 + \|\boldsymbol{s}_1\|^2 \\ \vdots \\ \left(\tilde{r}_{tN1} + L_{N1}\right)^2 - \|\boldsymbol{s}_N\|^2 + \|\boldsymbol{s}_1\|^2 \end{bmatrix} \tag{26}$$

$$\boldsymbol{H}_{\text{PCL}} = -\begin{bmatrix} \left(\boldsymbol{t}^T - \boldsymbol{s}_1^T\right) & -\left(\tilde{r}_{t1} + L_1\right) \\ \left(\boldsymbol{s}_2^T - \boldsymbol{s}_1^T\right) & \left(\tilde{r}_{t21} + L_{21}\right) \\ \left(\boldsymbol{s}_3^T - \boldsymbol{s}_1^T\right) & \left(\tilde{r}_{t31} + L_{31}\right) \\ \vdots & \vdots \\ \left(\boldsymbol{s}_N^T - \boldsymbol{s}_1^T\right) & \left(\tilde{r}_{tN1} + L_{N1}\right) \end{bmatrix} \tag{27}$$

$$\boldsymbol{\delta}_{\text{PCL}} = \begin{bmatrix} n_{\text{PCL},1} \\ \delta_{\text{PCL},2} \\ \delta_{\text{PCL},3} \\ \vdots \\ \delta_{\text{PCL},N} \end{bmatrix} \tag{28}$$

$$\begin{aligned} \boldsymbol{B}_{\text{PCL}} = \textbf{diag}\ &\left(\left[\left(\tilde{r}_{t1} + L_1\right) - r_1, \left(\tilde{r}_{t21} + L_{21}\right)\right.\right. \\ &\left.\left. + r_1, \ldots, \left(\tilde{r}_{tN1} + L_{N1}\right) + r_1\right]\right), \end{aligned} \tag{29}$$

and $\boldsymbol{\delta}_{\text{PCL}} \in \mathbb{R}^{N\times 1}$ is a zero-mean Gaussian vector with covariance matrix

$$\begin{aligned} \boldsymbol{Q}_{\text{PCL}} &= \mathbb{E}\left[\boldsymbol{\delta}_{\text{PCL}}\boldsymbol{\delta}_{\text{PCL}}^T\right] \\ &= \begin{bmatrix} \sigma^2_{\text{PCL}} & -\sigma^2_{\text{PCL}}\mathbf{1}^T_{N-1} \\ -\sigma^2_{\text{PCL}}\mathbf{1}_{N-1} & \sigma^2_{\text{PCL}}\left[\boldsymbol{I}_{N-1} + \mathbf{1}_{N-1}\mathbf{1}^T_{N-1}\right] \end{bmatrix}. \end{aligned} \tag{30}$$

C. Hybrid TDOA/PCL System Model

Exploiting (7) and (25), the hybrid TDOA/PCL measurement model[2] can be formulated as

$$\boldsymbol{a}_{\text{HYB}} - \boldsymbol{H}_{\text{HYB}}\boldsymbol{\theta} = \boldsymbol{B}_{\text{HYB}}\boldsymbol{\delta}_{\text{HYB}}, \tag{31}$$

where

[2]Note that, in this paper it is assumed an ideal detection process ($P_{\text{d}} = 1$ and $P_{\text{fa}} = 0$ for all the sensors) and a perfect association between measurements and corresponding targets.

$$\boldsymbol{a}_{\text{HYB}} = \begin{bmatrix} \boldsymbol{a}_{\text{TDOA}} \\ \boldsymbol{a}_{\text{PCL}} \end{bmatrix}, \tag{32}$$

$$\boldsymbol{H}_{\text{HYB}} = \begin{bmatrix} \boldsymbol{H}_{\text{TDOA}} \\ \boldsymbol{H}_{\text{PCL}} \end{bmatrix}, \tag{33}$$

$$\boldsymbol{B}_{\text{HYB}} = \begin{bmatrix} \boldsymbol{B}_{\text{TDOA}} & \boldsymbol{0} \\ \boldsymbol{0} & \boldsymbol{B}_{\text{PCL}} \end{bmatrix}, \tag{34}$$

$$\boldsymbol{\delta}_{\text{HYB}} = \begin{bmatrix} \boldsymbol{\delta}_{\text{TDOA}} \\ \boldsymbol{\delta}_{\text{PCL}} \end{bmatrix}. \tag{35}$$

$\boldsymbol{\delta}_{\text{HYB}}$ is a zero-mean Gaussian vector with covariance matrix

$$\boldsymbol{Q}_{\text{HYB}} = \begin{bmatrix} \boldsymbol{Q}_{\text{TDOA}} & \boldsymbol{0} \\ \boldsymbol{0} & \boldsymbol{Q}_{\text{PCL}} \end{bmatrix}. \tag{36}$$

III. CRLB

Applying Slepian-Bangs formula [32] to the the available measurements (5), (18), and (23), the Fisher Information Matrix (FIM) can be written as

$$\boldsymbol{J} = \begin{bmatrix} \frac{\partial \boldsymbol{\mu}^T}{\partial x} \\ \\ \frac{\partial \boldsymbol{\mu}^T}{\partial y} \end{bmatrix} \boldsymbol{Q}^{-1} \left[\frac{\partial \boldsymbol{\mu}}{\partial x}, \frac{\partial \boldsymbol{\mu}}{\partial y} \right] \Bigg|_{x=x_e, y=y_e} = \boldsymbol{G}^T \boldsymbol{Q}^{-1} \boldsymbol{G}, \tag{37}$$

where $\partial\boldsymbol{\mu}/\partial x$ (respectively $\partial\boldsymbol{\mu}/\partial y$) denotes the column vector containing the partial derivatives of the noise-free observations with respect to the unknown parameter x (respectively y), $\boldsymbol{G} = \left[\frac{\partial \boldsymbol{\mu}}{\partial x}, \frac{\partial \boldsymbol{\mu}}{\partial y} \right] \Big|_{x=x_e, y=y_e}$, and $\boldsymbol{Q}$ is the covariance matrix of the interference impairing the measurements. Precisely, for the TDOA system, $\mu_i = \mu_{\text{TDOA},i} = \|\boldsymbol{s}_i - \boldsymbol{u}\| - \|\boldsymbol{s}_1 - \boldsymbol{u}\|$, $i = 2, \ldots, N$, $\boldsymbol{Q} = \boldsymbol{Q}_{\text{TDOA}}$, and $\boldsymbol{G} = \boldsymbol{G}_{\text{TDOA}}$ defined as

$$\boldsymbol{G}_{\text{TDOA}_{i,1}} = \frac{\partial \mu_{\text{TDOA},i}}{\partial x} = -\frac{(x_i - x)}{\|\boldsymbol{s}_i - \boldsymbol{u}\|} + \frac{(x_1 - x)}{\|\boldsymbol{s}_1 - \boldsymbol{u}\|}, \quad i = 2, \ldots, N, \tag{38}$$

$$\boldsymbol{G}_{\text{TDOA}_{i,2}} = \frac{\partial \mu_{\text{TDOA},i}}{\partial y} = -\frac{(y_i - y)}{\|\boldsymbol{s}_i - \boldsymbol{u}\|} + \frac{(y_1 - y)}{\|\boldsymbol{s}_1 - \boldsymbol{u}\|}, \quad i = 2, \ldots, N, \tag{39}$$

As to the PCL system, $\mu_i = \mu_{\text{PCL},i} = \|\boldsymbol{t} - \boldsymbol{u}\| + \|\boldsymbol{s}_i - \boldsymbol{u}\| - L_i$, $i = 1, \ldots, N$, and $\boldsymbol{Q} = \sigma^2_{\text{PCL}} \boldsymbol{I}_N$, and $\boldsymbol{G} = \boldsymbol{G}_{\text{PCL}}$ given by

$$\boldsymbol{G}_{\text{PCL}_{i-1,1}} = \frac{\partial \mu_{\text{PCL},i}}{\partial x} = -\frac{(x_t - x)}{\|\boldsymbol{t} - \boldsymbol{u}\|} - \frac{(x_i - x)}{\|\boldsymbol{s}_i - \boldsymbol{u}\|}, \quad i = 1, \ldots, N, \tag{40}$$

$$\boldsymbol{G}_{\text{PCL}_{i-1,2}} = \frac{\partial \mu_{\text{PCL},i}}{\partial y} = -\frac{(y_t - y)}{\|\boldsymbol{t} - \boldsymbol{u}\|} - \frac{(y_i - y)}{\|\boldsymbol{s}_i - \boldsymbol{u}\|}, \quad i = 1, \ldots, N, \tag{41}$$

Finally, for the hybrid system the matrix $\boldsymbol{G}$ assumes the form

$$\boldsymbol{G}_{\text{HYB}} = \begin{bmatrix} \boldsymbol{G}_{\text{TDOA}} \\ \boldsymbol{G}_{\text{PCL}} \end{bmatrix}. \tag{42}$$

and $\boldsymbol{Q} = \boldsymbol{Q}_{\text{HYB}}$. Additionally, in this case, the FIM can be computed as

$$\boldsymbol{J}_{\text{HYB}} = \boldsymbol{J}_{\text{TDOA}} + \boldsymbol{J}_{\text{PCL}}. \tag{43}$$

Notably, equation (43) implies that

$$\boldsymbol{J}^{-1}_{\text{HYB}} \preceq \boldsymbol{J}^{-1}_{\text{TDOA}}, \tag{44}$$

$$\boldsymbol{J}^{-1}_{\text{HYB}} \preceq \boldsymbol{J}^{-1}_{\text{PCL}}, \tag{45}$$

which means that the benchmark performance (given by the CRLB) of the hybrid TDOA/PCL system is better than or equal to that achieved using the single TDOA or PCL strategy.

A. Identifiability of the Localization Problem

This subsection is devoted to the study of local identifiability of the estimation problem associated with the hybrid system based on TDOA and PCL measurements.

Before proceeding further, it is worth pointing out that model identifiability is a necessary condition for any well-posed estimation problem. In fact, the absence of such property implies that at least two different source states produce the same probability distributions of the observables making impossible to learn the true state value[3]. When the aforementioned property holds true within a neighborhood of a given source state $\boldsymbol{u}^0$, the estimation problem is said local identifiable around $\boldsymbol{u}^0$ [33]. Evidently, local identifiability in all the possible source states is a necessary condition for model identifiability. The following proposition summarizes our main result concerning the identifiability issue related to passive hybrid localization problem.

Proposition 3.1: If there are at least three sensors, $\boldsymbol{s}_1$, $\boldsymbol{s}_2$, $\boldsymbol{s}_3$, such that:

- each of the four sets $\{\boldsymbol{s}_1, \boldsymbol{s}_2, \boldsymbol{s}_3\}$, $\{\boldsymbol{s}_1, \boldsymbol{s}_2, \boldsymbol{t}\}$, $\{\boldsymbol{s}_2, \boldsymbol{s}_3, \boldsymbol{t}\}$, $\{\boldsymbol{s}_1, \boldsymbol{s}_3, \boldsymbol{t}\}$ comprises non-collinear points of the plane;
- there exists a pair of distinct sensors $\left(\boldsymbol{s}^1, \boldsymbol{s}^2\right) \in \{\boldsymbol{s}_1, \boldsymbol{s}_2, \boldsymbol{s}_3\}^2$ so that the remaining sensor, $\boldsymbol{s}^3$ say,
  - is located outside the triangle defined by the points $\{\boldsymbol{t}, \boldsymbol{s}^1, \boldsymbol{s}^2\}$,
  - belongs to the half plane induced by the straight line passing through $\boldsymbol{s}^1$ and $\boldsymbol{s}^2$ and containing $\boldsymbol{t}$,

then the hybrid localization problem is locally identifiable for all the possible target locations.

Proof: The proof is given in Appendix A. ■

IV. Localization Algorithms

The observation models for TDOA, PCL, and hybrid TDOA/PCL, defined in (7), (25), and (31), respectively, can be expressed in the following general form

[3]It is worth pointing out that, in some situations, an ambiguous measure can be helpful to improve the quality of the overall positioning process when data fusion with other sensors outputs is performed.

$$\boldsymbol{a} - \boldsymbol{H\theta} = \boldsymbol{B\delta} = \boldsymbol{\phi}. \tag{46}$$

Starting from (46) and assuming $\boldsymbol{H}$ full-rank, different techniques can be employed to recover the unknown target position. Here, the following four algorithms are considered:

- Least Squares (LS);
- Constrained Least Squares (CLS) [27];
- Two-Step Estimation (TSE) [28];
- Iterative Constrained Least Squares (ICLS);

A. LS Strategy

The estimator $\widehat{\boldsymbol{\theta}}_{\text{LS}}$ of $\boldsymbol{\theta}$ is given by

$$\widehat{\boldsymbol{\theta}}_{\text{LS}} = \arg\min_{\boldsymbol{\theta}\in\mathbb{R}^3} \left\{\|\boldsymbol{H\theta} - \boldsymbol{a}\|^2\right\} = \left(\boldsymbol{H}^T\boldsymbol{H}\right)^{-1}\boldsymbol{H}^T\boldsymbol{a}. \tag{47}$$

B. CLS Strategy

Observing that the three components of the vector $\boldsymbol{\theta}$ are functionally dependent, i.e. $r_1 = \|\boldsymbol{u}\|$, it is of interest to consider the CLS estimate $\widehat{\boldsymbol{\theta}}_{\text{CLS}}$ of $\boldsymbol{\theta}$ which is given by [27]

$$\begin{aligned}\widehat{\boldsymbol{\theta}}_{\text{CLS}}(\lambda^\star) &= \arg\min_{\boldsymbol{\theta}\in\mathbb{R}^3} \left\{\|\boldsymbol{H\theta} - \boldsymbol{a}\|^2 :\ \boldsymbol{\theta}^T\boldsymbol{C\theta} = 0, r_1 \geq 0\right\} \\ &= \left(\boldsymbol{H}^T\boldsymbol{H} + \lambda^\star\boldsymbol{C}\right)^{-1}\boldsymbol{H}^T\boldsymbol{a},\end{aligned} \tag{48}$$

where

$$\boldsymbol{C} = \begin{bmatrix}1 & 0 & 0\\ 0 & 1 & 0\\ 0 & 0 & -1\end{bmatrix}. \tag{49}$$

and $\lambda^\star \in \mathbb{R}$ is to be chosen among the roots of $\widehat{\boldsymbol{\theta}}_{\text{CLS}}^T(\lambda^\star)\boldsymbol{C}\widehat{\boldsymbol{\theta}}_{\text{CLS}}(\lambda^\star) = 0$ according to the procedure developed in [27]. It relies on the solution of a specific fourth order polynomial equation.

C. TSE Strategy

Denoting by $\boldsymbol{\Psi}$ the covariance matrix of $\boldsymbol{\phi}$, i.e.,

$$\boldsymbol{\Psi} = \mathbb{E}\left[\boldsymbol{\phi}\boldsymbol{\phi}^T\right] = \boldsymbol{BQB}^T, \tag{50}$$

the TSE procedure provides an iterative estimate of the target position [28]. Specifically, assuming the knowledge of $\boldsymbol{Q}$, TSE first implements the following iterative procedure

$$\overline{\boldsymbol{\theta}}_{\text{TSE}}^{(k)} = \left[\boldsymbol{H}^T\left(\boldsymbol{\Psi}^{(k)}\right)^{-1}\boldsymbol{H}\right]^{-1}\boldsymbol{H}^T\left(\boldsymbol{\Psi}^{(k)}\right)^{-1}\boldsymbol{a}, \quad k = 0,\ldots,K, \tag{51}$$

where K is the maximum number of iterations, $\boldsymbol{\Psi}^{(0)} = \boldsymbol{Q}$ and $\boldsymbol{\Psi}^{(k)}$, $k \geq 1$, is estimated starting from $\overline{\boldsymbol{\theta}}_{\text{TSE}}^{(k-1)}$ (i.e., using the third component for the computation of $\boldsymbol{B}$). The algorithm iteratively updates $\overline{\boldsymbol{\theta}}_{\text{TSE}}^{(k)}$ until $\|\overline{\boldsymbol{\theta}}_{\text{TSE}}^{(k)} - \overline{\boldsymbol{\theta}}_{\text{TSE}}^{(k-1)}\| \leq \epsilon$, $k = 1,\ldots,K$, with $\epsilon \geq 0$, or the maximum number of iterations is reached.

The second step of TSE attempts to improve the estimation accuracy exploiting the dependency among the components of the vector $\boldsymbol{\theta}$ starting from the error vector $\boldsymbol{g}$ defined as

$$\boldsymbol{g} = \hat{\boldsymbol{\theta}}_{\text{TSE}} - \boldsymbol{G}\bar{\boldsymbol{\theta}}, \tag{52}$$

where

$$\hat{\boldsymbol{\theta}}_{\text{TSE}} = \left[\overline{\theta}^2_{\text{TSE}_1},\ \overline{\theta}^2_{\text{TSE}_2},\ \overline{\theta}^2_{\text{TSE}_3}\right]^T, \tag{53}$$

$$\bar{\boldsymbol{\theta}} = \left[\theta_1^2, \theta_2^2\right]^T, \tag{54}$$

$$\boldsymbol{G} = \begin{bmatrix}1 & 0\\ 0 & 1\\ 1 & 1\end{bmatrix}, \tag{55}$$

and $\overline{\boldsymbol{\theta}}_{\text{TSE}}$ is the final output of (51). Notice that, if $\boldsymbol{g} = \boldsymbol{0}$ the position of the target is directly obtained at the first step. However, errors inevitably affect $\overline{\boldsymbol{\theta}}_{\text{TSE}}$ which can be modeled as

$$\overline{\boldsymbol{\theta}}_{\text{TSE}} = \boldsymbol{\theta} + \boldsymbol{n}, \tag{56}$$

where $\boldsymbol{n} = [n_1, n_2, n_3]^T$ are the estimation errors at the first step. Substituting (56) in (52) and ignoring the terms n_1^2, n_2^2, n_3^2, the covariance matrix of the error vector $\boldsymbol{g}$ can be approximated as [28]

$$\boldsymbol{\Omega} = \mathbb{E}\left[\boldsymbol{g}\boldsymbol{g}^T\right] \approx 4\boldsymbol{DFD}, \tag{57}$$

where $\boldsymbol{D} = \textbf{diag}\left(\overline{\boldsymbol{\theta}}_{\text{TSE}}\right)$ and $\boldsymbol{F}$ is an approximation for the covariance matrix of $\overline{\boldsymbol{\theta}}_{\text{TSE}}$ [28]

$$\boldsymbol{F} \approx \left(\boldsymbol{H}^T\boldsymbol{\Psi}^{-1}\boldsymbol{H}\right)^{-1}, \tag{58}$$

with $\boldsymbol{\Psi}$ the matrix obtained evaluating (50) in correspondence of the last instance of (51). Modeling $\boldsymbol{g}$ as a Gaussian random vector, the unconstrained Maximum Likelihood Estimator (MLE) of $\boldsymbol{\theta}$, obtained minimizing $\left(\hat{\boldsymbol{\theta}}_{\text{TSE}} - \boldsymbol{G\theta}\right)\boldsymbol{\Omega}^{-1}\left(\hat{\boldsymbol{\theta}}_{\text{TSE}} - \boldsymbol{G\theta}\right)$ is given by

$$\widehat{\boldsymbol{\theta}} = \left(\boldsymbol{G}^T\boldsymbol{\Omega}^{-1}\boldsymbol{G}\right)^{-1}\boldsymbol{G}^T\boldsymbol{\Omega}^{-1}\hat{\boldsymbol{\theta}}_{\text{TSE}}. \tag{59}$$

Equation (59) gives the estimate related to the square value of the x and y target coordinates, respectively. Hence, the possible target locations are given by

$$\overline{\boldsymbol{u}}_{\text{TSE},k} = \left[(-1)^k\sqrt{|\widehat{\theta}_1|},\ (-1)^{(k^2+k+2)/2}\sqrt{|\widehat{\theta}_2|}\right]^T, \quad k = 1,\ldots,4. \tag{60}$$

Based on (2), (14), and (21), the final estimate (chosen among the four candidates in (60)) is selected as the one which gives the minimum square error χ_k, $k = 1,\ldots,4$, defined as

$$\chi_{\text{TDOA},k} = \sum_{i=2}^{N} \left(\|\boldsymbol{s}_i - \overline{u}_{\text{TSE},k}\| - \|\boldsymbol{s}_1 - \overline{u}_{\text{TSE},k}\| - \tilde{r}_{i1} \right)^2, \quad k = 1, \ldots, 4 \tag{61}$$

for TDOA system,

$$\chi_{\text{PCL},k} = \left[\left(\|\boldsymbol{t} - \overline{u}_{\text{TSE},k}\| + \|\boldsymbol{s}_1 - \overline{u}_{\text{TSE},k}\| - L_1 - \tilde{r}_{t1} \right) + \sum_{i=2}^{N} \left(\|\boldsymbol{s}_i - \overline{u}_{\text{TSE},k}\| - \|\boldsymbol{s}_1 - \overline{u}_{\text{TSE},k}\| - L_{i1} - \tilde{r}_{ti1} \right) \right]^2, \quad k = 1, \ldots, 4 \tag{62}$$

for PCL system, and

$$\chi_{\text{HYB},k} = \chi_{\text{TDOA},k} + \chi_{\text{PCL},k}, \quad k = 1, \ldots, 4 \tag{63}$$

for hybrid TDOA/PCL system.

D. ICLS Strategy

This is a new iterative procedure which at each recursion solves the problem

$$\begin{aligned} \widehat{\boldsymbol{\theta}}_{\text{ICLS}}^{(k)} &= \arg \min_{\boldsymbol{\theta} \in \mathbb{R}^3} \left\{ \left\| \left(\boldsymbol{\Psi}^{(k)} \right)^{-1/2} \boldsymbol{H}\boldsymbol{\theta} - \left(\boldsymbol{\Psi}^{(k)} \right)^{-1/2} \boldsymbol{a} \right\|^2 : \right. \\ &\quad \left. \boldsymbol{\theta}^T \boldsymbol{C} \boldsymbol{\theta} = 0, r_1 \geq 0 \right\} \\ &= \left(\boldsymbol{H}^T \left(\boldsymbol{\Psi}^{(k)} \right)^{-1} \boldsymbol{H} + \beta_k^\star \boldsymbol{C} \right)^{-1} \boldsymbol{H}^T \left(\boldsymbol{\Psi}^{(k)} \right)^{-1} \boldsymbol{a}, \\ &\quad k = 0, \ldots, K, \end{aligned} \tag{64}$$

where K is the maximum number of iterations, $\beta_k^\star \in \mathbb{R}$ is such that $\widehat{\boldsymbol{\theta}}_{\text{ICLS}}^{(k)^T}(\beta_k^\star) \boldsymbol{C} \widehat{\boldsymbol{\theta}}_{\text{ICLS}}^{(k)}(\beta_k^\star) = 0$ and $\widehat{\boldsymbol{\theta}}_{\text{ICLS},3}^{(k)}(\beta_k^\star) \geq 0$. The iterative technique to find the position estimate is the same as that in Section IV-C, with the initialization $\boldsymbol{B}^{(0)} = \boldsymbol{I}$ and the update $\boldsymbol{B}^{(k)}$, $k \geq 1$, obtained starting from $\widehat{\boldsymbol{\theta}}_{\text{ICLS}}^{(k-1)}$. The algorithm iteratively updates $\widehat{\boldsymbol{\theta}}_{\text{ICLS}}^{(k)}$ until $\left\| \widehat{\boldsymbol{\theta}}_{\text{ICLS}}^{(k)} - \widehat{\boldsymbol{\theta}}_{\text{ICLS}}^{(k-1)} \right\| \leq \epsilon$, $k = 1, \ldots, K$, with $\epsilon \geq 0$ or the maximum number of iterations is reached. Note that, the second step of the TSE is no longer required since the obtained solution directly fulfills condition (52).

V. Performance Assessment

The performance of the proposed hybrid TDOA/PCL system is assessed in comparison with classic TDOA or PCL techniques. To this end a 2D localization scenario with one omnidirectional broadcast transmitter of opportunity and 4 receiving sensor nodes is considered. Specifically, as shown in Figure 1, 3 sensor nodes are located at the vertices of an equilateral triangle with side equal to 500 m, the reference sensor is located at the origin of the system, and the transmitter of opportunity is located on the bisector of the third quadrant of the system 5 km far from the reference sensor. To show the benefits of the proposed hybrid TDOA/PCL system, two different analyses are conducted:

- CRLB maps, i.e., $\sqrt{\text{Tr}\left(\boldsymbol{J}^{-1}\right)}$ with $\boldsymbol{J}$ the appropriate FIM, for different values of σ_{TDOA} and σ_{PCL};
- RMSE of the estimated target position using LS, CLS, TSE, and ICLS algorithms for different values of σ_{TDOA} and σ_{PCL}.

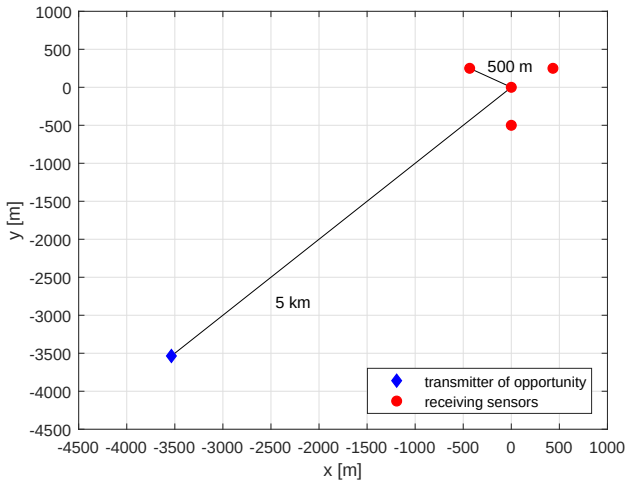

Figure 1. Geometric configuration of the sensor nodes and the transmitter of opportunity.

A. CRLB Analysis

CRLB for TDOA, PCL, and hybrid TDOA/PCL systems is compared for different values of σ_{TDOA} and σ_{PCL}. A grid of 10 square km (with a resolution of 25 m) centered at the reference sensor is considered and for each point CRLBs are computed. Figures 2(a), 2(b), and 3 show the CRLB maps obtained for $\sigma_{\text{TDOA}} = \sigma_{\text{PCL}} = 3$ m. The results highlight that the CRLB for PCL is significantly smaller than the CRLB for TDOA and the best performance is achieved jointly exploiting both TDOA and PCL measurements. Furthermore, given $\sigma_{\text{TDOA}} = 3$ m and increasing σ_{PCL}, the performance gap between conventional PCL and hybrid TDOA/PCL becomes larger and larger. This behaviour is shown in Figures 4(a) and 4(b) where the CRLB maps for conventional PCL and hybrid TDOA/PCL are evaluated considering $\sigma_{\text{TDOA}} = 3$ m and $\sigma_{\text{PCL}} = 30$ m. The analysis herein conducted highlights that the TDOA shows severe theoretical performance losses with respect to both PCL and hybrid approaches. Therefore, just the hybrid architecture and the standard PCL system are considered in subsequent analysis in terms of RMSE.

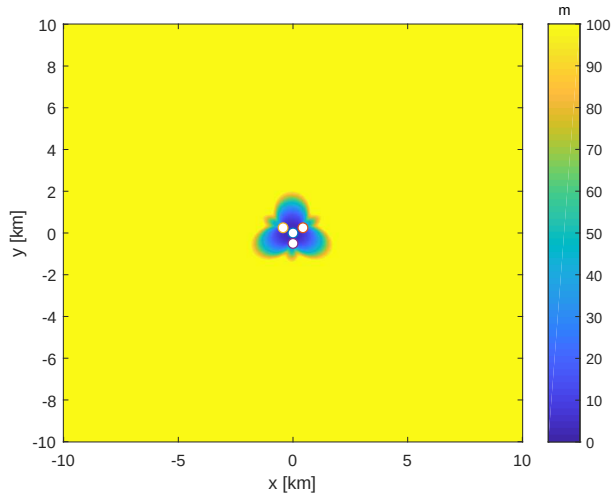

(a)

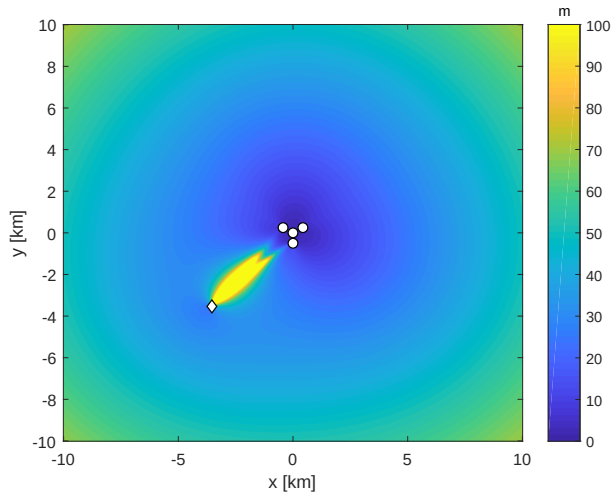

(b)

Figure 2. CRLB maps for TDOA (a) and PCL (b) systems considering $\sigma_{\text{TDOA}} = \sigma_{\text{PCL}} = 3$ m.

B. RMSE Analysis

Performance of PCL and hybrid TDOA/PCL systems are compared considering as figure of merit the RMSE of the estimated position using LS, CLS, TSE, and ICLS algorithms. For each strategy the RMSE is evaluated resorting to Monte Carlo simulation based on 10^5 independent trials. The true position of the target is $[x_e, y_e] = 5[\cos(\pi/8), \sin(\pi/8)]$ km and different values of σ_{TDOA} and σ_{PCL} are considered.

Figures 5 and 6 show the RMSE curves versus σ_{TDOA} assuming $\sigma_{\text{PCL}} = 5$ m and 25 m, respectively. For both study cases, results highlight that the LS algorithm achieves the worst performance, whereas the TSE algorithm ensures an RMSE almost overlapped with the corresponding CRLB. Furthermore, Figure 5 highlights that the TSE algorithm for hybrid TDOA/PCL uniformly outperforms all the PCL-based

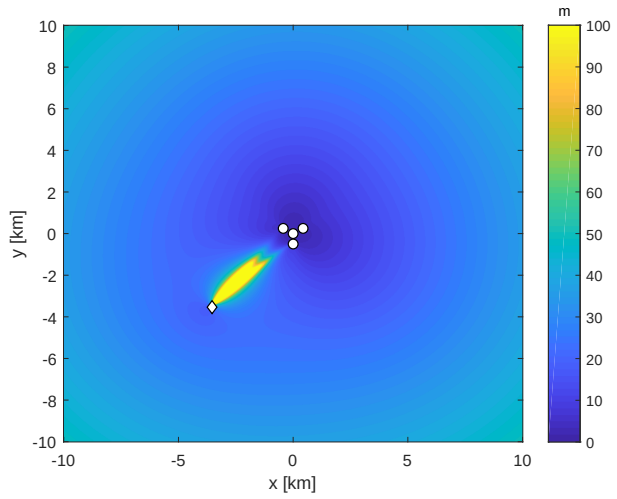

Figure 3. CRLB for hybrid TDOA/PCL system considering $\sigma_{\text{TDOA}} = \sigma_{\text{PCL}} = 3$ m.

competitors. As to the LS and CLS, there exists a threshold for σ_{TDOA}, $\bar{\sigma}_{\text{TDOA}}$ say, such that the hybrid framework can improve the PCL performance as long as $\sigma_{\text{TDOA}} \leq \bar{\sigma}_{\text{TDOA}}$. Nevertheless, the results of Figure 6 reveal that increasing σ_{PCL} the joint exploitation of TDOA and PCL measurements leads to more reliable estimates of the target position than the conventional PCL strategy regardless of the considered estimation algorithm. As to the ICLS, it shows performance comparable with the TSE for the hybrid system, even if for not all the considered σ_{TDOA} values; in fact, in some cases, it tends to have some performance losses with respect to both the TSE and CLS techniques. Moreover, analyzing the curves of subplots (b), the evidence is that when the ICLS is applied to a PCL system only, it has poor performances, with RMSE values close to those shown by the LS algorithm.

VI. Conclusions

A non-cooperative target position estimation technique jointly exploiting hyperbolic and elliptic passive location measurements has been proposed. Specifically, considering a passive sensor network where each node is equipped with a TDOA and a PCL receiver within a scenario with single transmitter of opportunity, the mathematical model for the joint exploitation of TDOA and PCL observations has been formulated. Then, CRLBs for TDOA, PCL and hybrid TDOA/PCL localization have been given together with some estimation algorithms for the cartesian coordinates of the target. At the analysis stage, results have shown the performance gains achievable using the proposed hybrid localization framework over classic TDOA or PCL systems.

Possible future researches might concern the study of the impact of a non-ideal detection process ($P_{\text{d}} < 1$ and $P_{\text{fa}} > 0$) as well as the development of appropriate techniques to overcome this drawback, the definition of advanced association strategies,

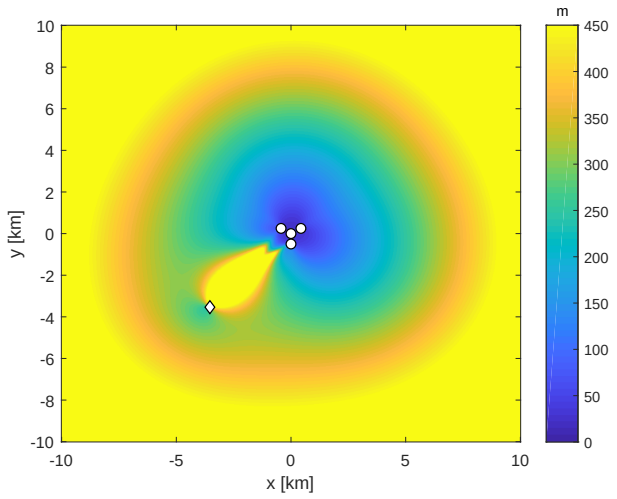

(a)

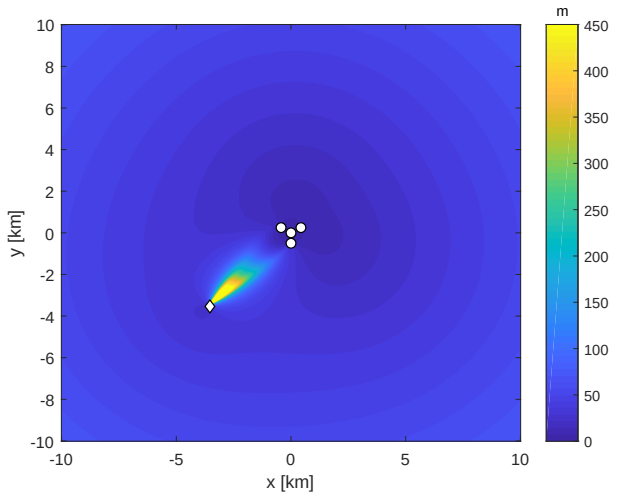

(b)

Figure 4. CRLB maps for PCL (a) and hybrid TDOA/PCL (b) systems considering $\sigma_{\text{TDOA}} = 3$ m and $\sigma_{\text{PCL}} = 30$ m.

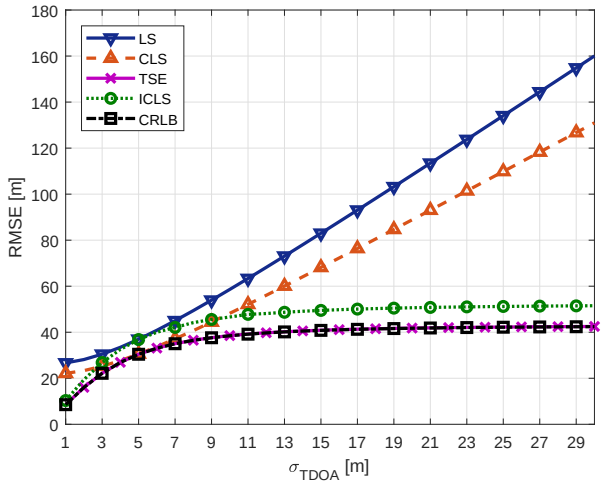

(a) Hybrid

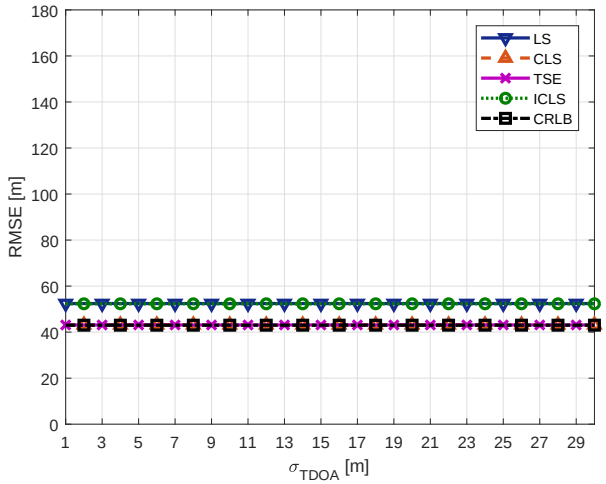

(b) PCL

Figure 5. RMSE vs σ_{TDOA} assuming $\sigma_{\text{PCL}} = 5$ m. Subplot (a) refers to the hybrid system, whereas subplot (b) to the PCL.

and the design of algorithms for sensors deployment optimization. It is also worth to consider TDOA and PCL receivers not necessarily co-located as well as the design of robust strategies accounting for some uncertainty in the position of the receiving sensor nodes. Moreover, the effect of jamming on localization performance could be also studied [34]. Finally, it would be definitely interesting to assess the performance of the hybrid localization algorithms in the presence of real measured data.

ACKNOWLEDGMENT

The authors would like to thank the Editor and the Referees for the interesting questions and comments that have helped to improve this paper.

APPENDIX

A. *Proof of Proposition 3.1*

Before proceeding with the proof of the proposition, some relevant and useful results available in the open literature are now reported [33].

Let us consider a random vector $\boldsymbol{x}$ in $\mathbb{R}^L$, whose probability density function (pdf) belongs to a family of functions parametrized by vector a $\boldsymbol{u} \in \mathbb{R}^M$. Precisely, at each $\boldsymbol{u} \in \mathcal{A} \subseteq \mathbb{R}^M$, with $\mathcal{A}$ the source state space, it is associated a continuous pdf $f(\boldsymbol{x}; \boldsymbol{u})$.

Definition A.1: A parameter point $\boldsymbol{u}^0 \in \mathcal{A}$ is said to be locally identifiable if there exists an open neighborhood $\mathcal{I}_{\boldsymbol{u}^0}$ of $\boldsymbol{u}^0$ containing no other $\boldsymbol{u}$ in $\mathcal{I}_{\boldsymbol{u}^0} \cap \mathcal{A}$ which is observationally

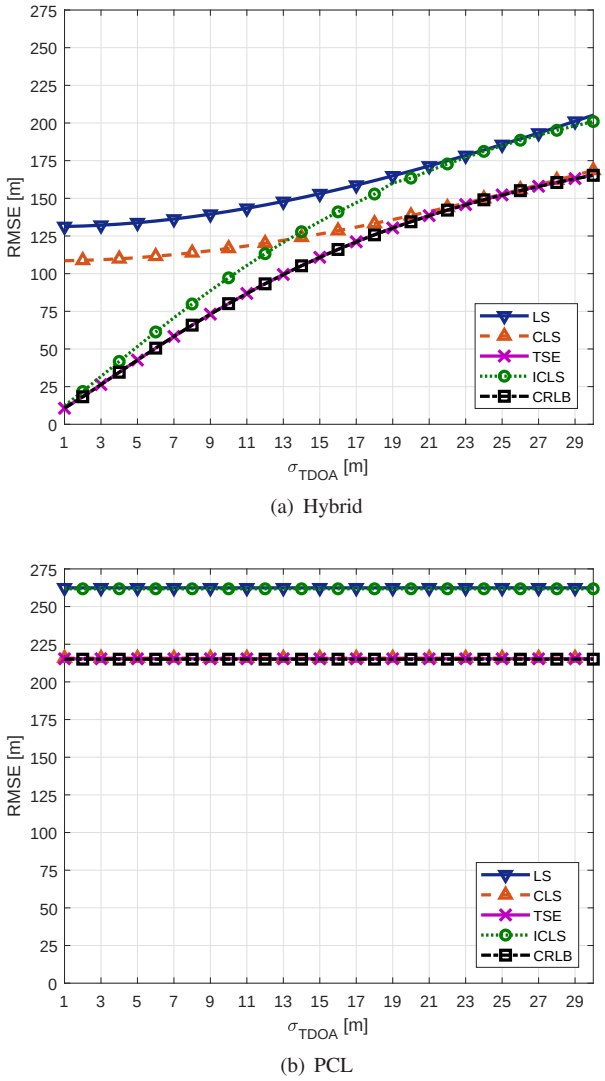

(a) Hybrid

(b) PCL

Figure 6. RMSE vs σ_{TDOA} assuming $\sigma_{\text{PCL}} = 25$ m. Subplot (a) refers to the hybrid system, whereas subplot (b) to the PCL.

equivalent[4] to $\boldsymbol{u}^0$ [33].

The following lemma summarizes the main technical result concerning the local identifiability issue related to an estimation problem [33], [35].

Lemma A.2: Let $\boldsymbol{u}^0$ be a regular point[5] of the FIM $\boldsymbol{J}(\boldsymbol{u})$. Then, $\boldsymbol{u}^0$ is locally identifiable if and only if $\boldsymbol{J}(\boldsymbol{u}^0)$ is non singular [33, Theorem 1].

From Lemma A.2, being the FIM in (37) a continuous function in $\mathbb{R}^2$ apart from the closed set $\{\boldsymbol{t}, \boldsymbol{s}_1, \ldots, \boldsymbol{s}_N\}$, it can be claimed that a sufficient condition to ensure the local identifiability of the considered localization problem is that the FIM in (37) is invertible, i.e.,

$$\det(\boldsymbol{J}) = \det\left(\boldsymbol{G}_{\text{HYB}}^T \begin{bmatrix} \boldsymbol{Q}_{\text{TDOA}}^{-1} & \boldsymbol{0} \\ \boldsymbol{0} & \boldsymbol{Q}_{\text{PCL}}^{-1} \end{bmatrix} \boldsymbol{G}_{\text{HYB}}\right) > 0. \quad (65)$$

Therefore, the local identifiability of the localization problem can be studied by means of the rank of the matrix

$$\begin{aligned} \text{Rank}\left(\boldsymbol{P}^T\boldsymbol{P}\right) &= \text{Rank}\left(\boldsymbol{P}\right) = \text{Rank}\left(\boldsymbol{Q}^{-1/2}\boldsymbol{G}_{\text{HYB}}\right) \\ &= \text{Rank}\left(\boldsymbol{G}_{\text{HYB}}\right), \end{aligned} \quad (66)$$

where

$$\boldsymbol{P} = \begin{bmatrix} \boldsymbol{Q}_{\text{TDOA}}^{-1/2} & \boldsymbol{0} \\ \boldsymbol{0} & \boldsymbol{Q}_{\text{PCL}}^{-1/2} \end{bmatrix} \boldsymbol{G}_{\text{HYB}}.$$

From (42) and (66), it follows that (for any point where the FIM is well-defined) if at least one between $\boldsymbol{G}_{\text{PCL}}$ and $\boldsymbol{G}_{\text{TDOA}}$ is rank-2 then $\boldsymbol{G}_{\text{HYB}}$ is full-rank too and local identifiability holds true. In the following, to avoid redundancies, the identifibility study is conducted with reference to the PCL system, whereas the final result is directly given for the TDOA counterpart without any explicit proof.

To proceed further, let us observe that the identifiability issue of a PCL system with N sensors, corresponding to a matrix $\boldsymbol{G}_{\text{PCL}}$ of size $N \times 2$ matrix, can be carried out analyzing all the sensing configurations composed of a transmitter of opportunity and all the possible different pairs of sensors. To this end, note that if for a specific point in $\mathbb{R}^2$ it can be ensured the existence of a PCL system with 2 sensors for which the resulting matrix $\boldsymbol{G}_{\text{PCL}}$ is rank-2, then the problem is locally identifiable in that specific point. Indeed, the above condition guarantees that there exists a neighborhood of that point such that the overall system of equations associated with the PCL-based localization problem at hand admits a unique solution.

1) Rank of $\boldsymbol{G}_{PCL}$ for a configuration with 2 sensors: the considered configuration comprises a transmitter of opportunity, $\boldsymbol{t}$, and two sensors, $\boldsymbol{s}_1$ and $\boldsymbol{s}_2$, with $\{\boldsymbol{t}, \boldsymbol{s}_1, \boldsymbol{s}_2\}$ non-collinear. Moreover, without loss of generality, let us assume that $\boldsymbol{s}_1 = [0, 0]^T$, i.e., $\boldsymbol{s}_1$ is located at the center of the reference system.

Based om previous considerations, the goal is to study the rank of the matrix

$$\boldsymbol{G}_{\text{PCL}} = \left[\frac{\boldsymbol{u}}{\|\boldsymbol{u}\|} - \frac{\boldsymbol{t}-\boldsymbol{u}}{\|\boldsymbol{t}-\boldsymbol{u}\|}, \frac{\boldsymbol{u}-\boldsymbol{s}_2}{\|\boldsymbol{u}-\boldsymbol{s}_2\|} - \frac{\boldsymbol{t}-\boldsymbol{u}}{\|\boldsymbol{t}-\boldsymbol{u}\|}\right] \quad (67)$$

for all the target positions different from $\boldsymbol{s}_1, \boldsymbol{s}_2$ and $\boldsymbol{t}$. To this end, two distinct conditions (associated to the target location) are considered and analyzed in the following: the former assumes that $\boldsymbol{u}$ is such that $\frac{\boldsymbol{u}}{\|\boldsymbol{u}\|}$ and $\frac{\boldsymbol{u}-\boldsymbol{s}_2}{\|\boldsymbol{u}-\boldsymbol{s}_2\|}$ are linearly dependent (**Case A**); the latter comprises the location points for which $\frac{\boldsymbol{u}}{\|\boldsymbol{u}\|}$ and $\frac{\boldsymbol{u}-\boldsymbol{s}_2}{\|\boldsymbol{u}-\boldsymbol{s}_2\|}$ are linearly independent (**Case B**).

- **Case A:** If $\frac{\boldsymbol{u}}{\|\boldsymbol{u}\|}$ and $\frac{\boldsymbol{u}-\boldsymbol{s}_2}{\|\boldsymbol{u}-\boldsymbol{s}_2\|}$ are linearly dependent, then

$$\frac{\boldsymbol{u}}{\|\boldsymbol{u}\|} = \lambda\frac{\boldsymbol{u}-\boldsymbol{s}_2}{\|\boldsymbol{u}-\boldsymbol{s}_2\|}, \quad (68)$$

with $\lambda = \pm 1$, since they are unitary norm vectors.

[4]Two parameter points (structures) $\boldsymbol{u}^1$ and $\boldsymbol{u}^2$ are said to be observationally equivalent if $f(\boldsymbol{x}, \boldsymbol{u}^1) = f(\boldsymbol{x}, \boldsymbol{u}^2)$ for all $\boldsymbol{x}$ in $\mathbb{R}^L$ [33].

[5]Let $\boldsymbol{M}(\boldsymbol{u})$ be a matrix whose elements are continuous functions of $\boldsymbol{u}$ everywhere in $\mathcal{A}$ (open set in $\mathbb{R}^M$). The point $\boldsymbol{u}^0 \in \mathcal{A}$ is said to be a regular point of the matrix if there exists an open neighborhood of $\boldsymbol{u}^0$ in which $\boldsymbol{M}(\boldsymbol{u})$ has constant rank [33].

In this situation, the following two sub-cases can be distinguished:

[A.1]: for $\lambda = 1$, it immediately follows that Rank $(\boldsymbol{G}_{\text{PCL}}) = 1$; such condition corresponds to the point of $\mathbb{R}^2$

$$\boldsymbol{u} = \frac{1}{1 - \frac{\|\boldsymbol{u}-\boldsymbol{s}_2\|}{\|\boldsymbol{u}\|}} \boldsymbol{s}_2 \;\Rightarrow\; \boldsymbol{u} = \alpha \boldsymbol{s}_2, \tag{69}$$

with $\alpha < 0$ or $\alpha > 1$.

[A.2]: for $\lambda = -1$, the matrix $\boldsymbol{G}_{\text{PCL}}$ reduces to

$$\boldsymbol{G}_{\text{PCL}} = \left[\frac{\boldsymbol{u}}{\|\boldsymbol{u}\|} - \frac{\boldsymbol{t}-\boldsymbol{u}}{\|\boldsymbol{t}-\boldsymbol{u}\|}, -\frac{\boldsymbol{u}}{\|\boldsymbol{u}\|} - \frac{\boldsymbol{t}-\boldsymbol{u}}{\|\boldsymbol{t}-\boldsymbol{u}\|} \right].$$

Now, note that the target locations $\boldsymbol{u}$ fulfilling (68) with $\lambda = -1$ describe the line segment connecting $\boldsymbol{s}_1$ and $\boldsymbol{s}_2$. Being, by assumption, $\boldsymbol{s}_1$, $\boldsymbol{s}_2$, and $\boldsymbol{t}$ not-aligned, then $\boldsymbol{t}-\boldsymbol{u}$ and $\boldsymbol{u}$ are not-aligned and in this case $\boldsymbol{G}_{\text{PCL}}$ has rank-2.

- **Case B:** If $\frac{\boldsymbol{u}}{\|\boldsymbol{u}\|}$ and $\frac{\boldsymbol{u}-\boldsymbol{s}_2}{\|\boldsymbol{u}-\boldsymbol{s}_2\|}$ are linearly independent, then applying Lemma A.4 with $\boldsymbol{a} = \frac{\boldsymbol{u}}{\|\boldsymbol{u}\|}$ and $\boldsymbol{b} = \frac{\boldsymbol{u}-\boldsymbol{s}_2}{\|\boldsymbol{u}-\boldsymbol{s}_2\|}$, the matrix $\boldsymbol{G}$ has rank 1 if and only if $\frac{\boldsymbol{t}-\boldsymbol{u}}{\|\boldsymbol{t}-\boldsymbol{u}\|}$ belongs to the straight line passing through $\frac{\boldsymbol{u}}{\|\boldsymbol{u}\|}$ and $\frac{\boldsymbol{u}-\boldsymbol{s}_2}{\|\boldsymbol{u}-\boldsymbol{s}_2\|}$. This is possible if and only if:

[B.1]: the point $(\boldsymbol{t}-\boldsymbol{u})/\|\boldsymbol{t}-\boldsymbol{u}\|$ is equal to the first extreme $\boldsymbol{u}/\|\boldsymbol{u}\|$. As a consequence

$$\boldsymbol{u} = \frac{\frac{\|\boldsymbol{u}\|}{\|\boldsymbol{t}-\boldsymbol{u}\|}}{1 + \frac{\|\boldsymbol{u}\|}{\|\boldsymbol{t}-\boldsymbol{u}\|}} \boldsymbol{t} \;\Rightarrow\; \boldsymbol{u} = \alpha \boldsymbol{t}, \tag{70}$$

with $0 < \alpha < 1$.

[B.2]: the point $(\boldsymbol{t}-\boldsymbol{u})/\|\boldsymbol{t}-\boldsymbol{u}\|$ is equal to the second extreme $(\boldsymbol{u}-\boldsymbol{s}_2)/\|\boldsymbol{u}-\boldsymbol{s}_2\|$. As a consequence

$$\begin{aligned} \boldsymbol{u} &= \frac{1}{1 + \frac{\|\boldsymbol{t}-\boldsymbol{u}\|}{\|\boldsymbol{u}-\boldsymbol{s}_2\|}} \boldsymbol{t} + \frac{\frac{\|\boldsymbol{t}-\boldsymbol{u}\|}{\|\boldsymbol{u}-\boldsymbol{s}_2\|}}{1 + \frac{\|\boldsymbol{t}-\boldsymbol{u}\|}{\|\boldsymbol{u}-\boldsymbol{s}_2\|}} \boldsymbol{s}_2 \\ &\Rightarrow\; \boldsymbol{u} = \alpha \boldsymbol{t} + \beta \boldsymbol{s}_2, \end{aligned} \tag{71}$$

with $0 < \alpha < 1$ and $\alpha + \beta = 1$.

Summarizing, in Figure 7, the points in the 2D space where the PCL system is non identifiable are shown for a configuration with 2 sensors and a transmitter of opportunity.

Remark A.3: Let us now focus on a PCL system with a transmitter of opportunity and 3 receiving sensors assuming that a third sensor $\boldsymbol{s}_3$ is added to the sensing configuration of Figure 7; in particular, the points $\boldsymbol{t}, \boldsymbol{s}_1, \boldsymbol{s}_2, \boldsymbol{s}_3$ are supposed triple by triple not-aligned. Now, if $\boldsymbol{s}_3$ is placed outside the triangle defined by the points $\{\boldsymbol{t}, \boldsymbol{s}_1, \boldsymbol{s}_2\}$ and $\boldsymbol{s}_3$ belongs to the half plane induced by the straight line passing through $\boldsymbol{s}_1$ and $\boldsymbol{s}_2$ and containing $\boldsymbol{t}$, then it is always possible to find a configuration made by the transmitter and 2 appropriate sensors such that the problem is locally identifiable also along the (previously non-identifiable) line segments departing from the remaining sensor (but for the point $\boldsymbol{t}$). As a result, the only point for a PCL system with a transmitter of opportunity and 3 receiving sensors deployed in such a way where identifiability can not be claimed is just the transmitter location.

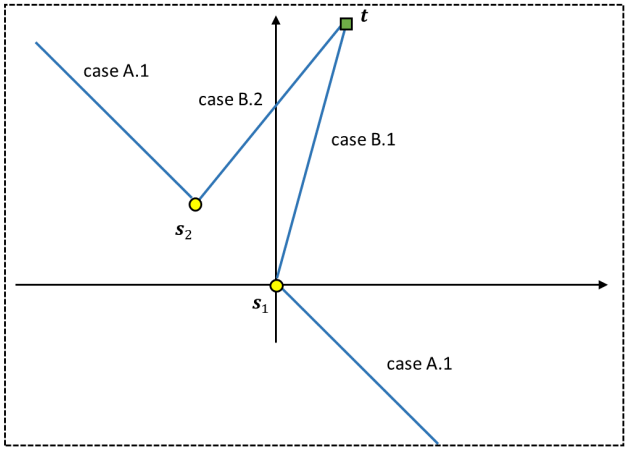

Figure 7. Geometric representation of the region of locally identifiable states for the PCL system in the 2D space and a configuration with a transmitter of opportunity and 2 receiving sensors (not-aligned).

Concluding, it can be claimed that sufficient condition to ensure the local identifiability for the PCL system, except for the transmitter location, is to deploy three sensors according to the configuration depicted in Remark A.3.

2) Rank of $\boldsymbol{G}_{TDOA}$ for a configuration with 3 sensors: the feasibility study for the TDOA system is similar to that described for the PCL. Precisely, 3 not-aligned sensors ensure the identifiability of the location problem for all the points except for those on the straight lines passing through each pair of sensors and external to the segments connecting them, i.e. (assuming $\boldsymbol{s}_1 = [0,0]^T$),

[C.1]: $\boldsymbol{u} = \boldsymbol{s}_2 + \alpha(\boldsymbol{s}_3 - \boldsymbol{s}_2)$, with $\alpha < 0$ or $\alpha > 1$.
[C.2]: $\boldsymbol{u} = \alpha \boldsymbol{s}_2$, with $\alpha < 0$ or $\alpha > 1$.
[C.3]: $\boldsymbol{u} = \alpha \boldsymbol{s}_3$, with $\alpha < 0$ or $\alpha > 1$.

In Figure 8, the points where TDOA is non identifiable in a 2D space for a configuration with 3 not-aligned sensors is pictorially represented. Hence, a sufficient condition for the local identifiability of a PCL system is to place a fourth sensor inside the triangle defined by $\{\boldsymbol{s}_1, \boldsymbol{s}_2, \boldsymbol{s}_3\}$.

3) Rank of $\boldsymbol{G}$ for a hybrid system: to evaluate the rank of $\boldsymbol{G}_{\text{HYB}}$ for the general hybrid system, the results obtained for isolated PCL and TDOA can be invoked. Precisely, from Remark A.3 it follows that the PCL with one transmitter and 3 sensors triple by triple not-aligned and deployed according to the strategy given in Remark A.3 ensures the local identifiability in $\mathbb{R}^2$ except for the transmitter location; however, the 3 not-aligned receiving TDOA sensor configuration ensures the identifiability at the PCL-transmitter location and the proof of the proposition is completed.

B. Lemma on Linear Dependence of Vectors

Lemma A.4: Let $\boldsymbol{a}$ and $\boldsymbol{b}$ two linearly independent vectors $\in \mathbb{R}^2$. Then, $(\boldsymbol{a}-\boldsymbol{c})$ and $(\boldsymbol{b}-\boldsymbol{c})$ are linearly dependent if and

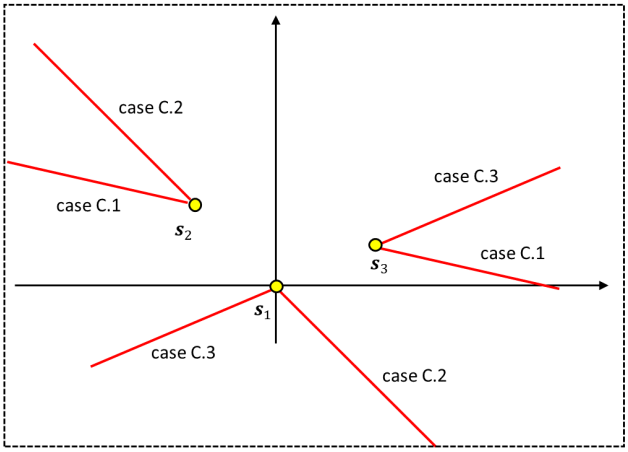

Figure 8. Geometric representation of the region of locally identifiable states for the TDOA system in a 2D space and a configuration with 3 not-aligned sensors.

only if $\boldsymbol{c}$ is a point on the straight line passing through $\boldsymbol{a}$ and $\boldsymbol{b}$.

Proof: The vectors $(\boldsymbol{a}-\boldsymbol{c})$ and $(\boldsymbol{b}-\boldsymbol{c})$ are linearly dependent if and only if $\exists\,(\alpha_1,\alpha_2)\neq(0,0)$ such that the linear combination $\alpha_1(\boldsymbol{a}-\boldsymbol{c})+\alpha_2(\boldsymbol{b}-\boldsymbol{c})=0$. The latter condition is equivalent to

$$\boldsymbol{c}=\boldsymbol{a}\frac{\alpha_1}{\alpha_1+\alpha_2}+\boldsymbol{b}\left(1-\frac{\alpha_1}{\alpha_1+\alpha_2}\right)=\boldsymbol{b}+\beta\,(\boldsymbol{a}-\boldsymbol{b})\,. \quad (72)$$

■

REFERENCES

[1] D. J. Torrieri, "Statistical Theory of Passive Location Systems," *IEEE Transactions on Aerospace and Electronic Systems*, vol. 20, no. 2, pp. 183–198, March 1984.

[2] B. Friedlander, "A Passive Localization Algorithm and its Accuracy Analysis," *IEEE Journal of Oceanic Engineering*, vol. 12, no. 1, pp. 234–245, January 1987.

[3] L. Cong and W. Zhuang, "Hybrid TDOA/AOA Mobile User Location for Wideband CDMA Cellular Systems," *IEEE Transactions on Wireless Communications*, vol. 1, no. 3, pp. 439–447, July 2002.

[4] H. D. Griffiths, C. J. Baker, H. Ghaleb, R. Ramakrishnan, and E. Willman, "Measurement and Analysis of Ambiguity Functions of Off-Air Signals for Passive Coherent Location," *Electronics Letters*, vol. 39, no. 13, pp. 1005–1007, June 2003.

[5] K. C. Ho and W. Xu, "An Accurate Algebraic Solution for Moving Source Location using TDOA and FDOA Measurements," *IEEE Transactions on Signal Processing*, vol. 52, no. 9, pp. 2453–2463, September 2004.

[6] J. M. Thomas, H. D. Griffiths, and C. J. Baker, "Ambiguity Function Analysis of Digital Radio Mondiale Signals for HF Passive Bistatic Radar," *Electronics Letters*, vol. 42, no. 25, pp. 1482–1483, December 2006.

[7] P. E. Howland, H. D. Griffiths, and C. J. Baker, *Bistatic Radar: Emerging Technology (M. Cherniakov ed.)*, chapter Passive Bistatic Radar, Wiley, New York, 2008.

[8] P. Falcone, F. Colone, A. Macera, and P. Lombardo, "Two-Dimensional Location of Moving Targets Within Local Areas using WiFi-Based Multistatic Passive Radar," *IET Radar, Sonar and Navigation*, vol. 8, no. 2, pp. 123–131, February 2014.

[9] V. Anastasio, A. Farina, F. Colone, and P. Lombardo, "Cramér-Rao Lower Bound with Pd $<$ 1 for Target Localisation Accuracy in Multistatic Passive Radar," *IET Radar, Sonar and Navigation*, vol. 8, no. 7, pp. 767–775, August 2014.

[10] D. Pastina, F. Colone, T. Martelli, and P. Falcone, "Parasitic Exploitation of Wi-Fi Signals for Indoor Radar Surveillance," *IEEE Transactions on Vehicular Technology*, vol. 64, no. 4, pp. 1401–1415, April 2015.

[11] Y. T. Chan and K. C. Ho, "A Simple and Efficient Estimator for Hyperbolic Location," *IEEE Transactions on Signal Processing*, vol. 42, no. 8, pp. 1905–1915, August 1994.

[12] K. C. Ho and Y. T. Chan, "Solution and Performance Analysis of Geolocation by TDOA," *IEEE Transactions on Aerospace and Electronic Systems*, vol. 29, no. 4, pp. 1311–1322, October 1993.

[13] L. Rui and K. C. Ho, "Elliptic Localization: Performance Study and Optimum Receiver Placement," *IEEE Transactions on Signal Processing*, vol. 62, no. 18, pp. 4673–4688, September 2014.

[14] H. D. Griffiths and C. J. Baker, "Passive Coherent Location Radar Systems. Part 1: Performance Prediction," *IEE Proceedings - Radar, Sonar and Navigation*, vol. 152, no. 3, pp. 153–159, June 2005.

[15] H. Y. C. Hang Y.-T. Chan and P.-C. Ching, "Exact and Approximate Maximum Likelihood Localization Algorithms," *IEEE Transactions on Vehicular Technology*, vol. 55, no. 1, pp. 10–16, January 2006.

[16] M. Malanowski and K. Kulpa, "Two Methods for Target Localization in Multistatic Passive Radar," *IEEE Transactions on Aerospace and Electronic Systems*, vol. 48, no. 1, pp. 572–580, 2012.

[17] W. L. Melvin and J. A. Scheer, Eds., *Principles of Modern Radar: Radar Applications*, Schitech Publishing, 2014.

[18] M. Malanowski, K. Kulpa, J. Kulpa, P. Samczynski, and J. Misiurewicz, "Analysis of Detection Range of FM-Based Passive Radar," *IET Radar, Sonar Navigation*, vol. 8, no. 2, pp. 153–159, February 2014.

[19] H. Kuschel, F. Hoffmann, and A. Schroeder, *Novel Radar Techniques and Applications*, vol. 1, chapter Multi-Illuminator and Multistatic Passive Radar, Scitech publishing, 2017.

[20] D. Gromek, K. Kulpa, and P. Samczynski, "Experimental Results of Passive SAR Imaging Using DVB-T Illuminators of Opportunity," *IEEE Geoscience and Remote Sensing Letters*, vol. 13, no. 8, pp. 1124–1128, Aug 2016.

[21] C. Bongioanni, F. Colone, S. Bernardini, L. Lelli, A. Stavolo, and P. Lombardo, "Passive Radar Prototypes for Multifrequency Target Detection," *Proceedings of SPIE - The International Society for Optical Engineering*, 10 2007.

[22] H. Kuschel, J. Heckenbach, R. Appel, et al., "On the Potentials of Passive, Multistatic, Low Frequency Radars to Counter Stealth and Detect Low Flying Targets," in *IEEE Radar Conference*. IEEE, 2008, pp. 1–6.

[23] D. W. O'Hagan, H. Kuschel, and J. Schiller, "Passive Bistatic Radar Analysis," in *Photonics Applications in Astronomy, Communications, Industry, and High-Energy Physics Experiments 2009*. International Society for Optics and Photonics, 2009, vol. 7502.

[24] P. Howland, "Guest Editorial Special Issue on Passive Radar Systems," *IEE Proceedings on Radar, Sonar and Navigation*, vol. 152, no. 3, pp. 105–223, 2005.

[25] A. Farina and H. Kuschel, "Guest Editorial Special Issue on Passive Radar (Part I)," *IEEE Aerospace and Electronic Systems Magazine*, vol. 27, no. 10, pp. 5–59, 2012.

[26] F. Colone, *Novel Radar Techniques and Applications*, vol. 1, chapter Short-Range Passive Radar Potentialities, Scitech publishing, 2017.

[27] A. Beck, P. Stoica, and J. Li, "Exact and Approximate Solutions of Source Localization Problems," *IEEE Transactions on Signal Processing*, vol. 56, no. 5, pp. 1770–1778, May 2008.

[28] J. Shen, A. Molisch, and J. Salmi, "Accurate Passive Location Estimation Using TOA Measurements," *IEEE Transactions on Wireless Communications*, vol. 11, no. 6, pp. 2182–2192, June 2012.

[29] T. Brenner, P. Kasprzak, K. Kulpa, L. Lamentowski, and M. Malanowski, "The Benefits of Data Fusion from PCL and PET Passive Sensors," in *Proceedings of SET-187 Research Specialist Meeting, Passive Radar, Challenges concerning Theory and Practice in Military Applications, STO-MP-SET-187 AC/323(SET-187)/TP/513*.

[30] T. Brenner, P. Kasprzak, and L. Lamentowski, "Position Estimation in the Multiband PCL-PET Fusion System," in *15th International Radar Symposium (IRS)*, Gdansk, pp. 1–4.

[31] L. Lamentowski, R. Mularzuk, T. Brenner, and M. Nieszporski, "Tracking Algorithm Analysis for the PCL-PET Fusion System," in *Signal Processing Symposium (SPSympo)*, Debe, pp. 1–6.

[32] H. L. Van Trees, *Detection, Estimation, and Modulation Theory*, John Wiley & Sons, 2004.

[33] T. J. Rothenberg, "Identification in Parametric Models," *Econometrica: Journal of the Econometric Society*, pp. 577–591, 1971.

[34] S. Paine, D. W. O'Hagan, M. Inggs, C. Schupbach, and U. Boniger, "Evaluating the Performance of FM Based PCL Radar in the Presence of Jamming," *IEEE Transactions on Aerospace and Electronic Systems*, pp. 1–13, 2018.

[35] C. Jauffret, "Observability and Fisher Information Matrix in Nonlinear Regression," *IEEE Transactions on Aerospace and Electronic Systems*, vol. 43, no. 2, pp. 756–759, 2007.

Augusto Aubry (M'12, SM'16) received the Dr.Eng. degree (with honors) and the Ph.D. degree in information engineering, both from the University of Naples Federico II, Naples, Italy, in 2007 and 2011, respectively. From February to April 2012, he was a Visiting Researcher with the Hong Kong Baptist University, Hong Kong. He is currently under research agreement with the Department of Electrical and Information Technology Engineering, University of Naples Federico II. His research interests include statistical signal processing and optimization theory, with emphasis on MIMO communications and radar signal processing. Dr. Aubry is also the co-recipient of the 2013 best paper award (entitled to B. Carlton) of the IEEE Transactions on Aerospace and Electronic Systems with the contribution "Knowledge-Aided (Potentially Cognitive) Transmit Signal and Receive Filter Design in Signal-Dependent Clutter".

Vincenzo Carotenuto (S'12, M'16, SM'19) received the M.Sc. degree in telecommunication engineering and the Ph.D. degree in electronic and telecommunication engineering from the University of Naples Federico II, Naples, Italy, in 2010 and 2015, respectively. His research interest lies in the field of statistical signal processing, with an emphasis on radar signal processing. Dr. Carotenuto is also the co-recipient of the best radar paper award at the IEEE Metrology for Aerospace 2018.

Antonio De Maio (S'01-A'02-M'03-SM'07-F'13) was born in Sorrento, Italy, on June 20, 1974. He received the Dr.Eng. degree (with honors) and the Ph.D. degree in information engineering, both from the University of Naples Federico II, Naples, Italy, in 1998 and 2002, respectively. From October to December 2004, he was a Visiting Researcher with the U.S. Air Force Research Laboratory, Rome, NY. From November to December 2007, he was a Visiting Researcher with the Chinese University of Hong Kong, Hong Kong. Currently, he is a Professor with the University of Naples Federico II. His research interest lies in the field of statistical signal processing, with emphasis on radar detection, optimization theory applied to radar signal processing, and multiple-access communications. Dr. De Maio is the recipient of the 2010 IEEE Fred Nathanson Memorial Award as the young (less than 40 years of age) AESS Radar Engineer 2010 whose performance is particularly noteworthy as evidenced by contributions to the radar art over a period of several years, with the following citation for "robust CFAR detection, knowledge-based radar signal processing, and waveform design and diversity". Dr. De Maio is the co-recipient of the 2013 best paper award (entitled to B. Carlton) of the IEEE Transactions on Aerospace and Electronic Systems with the contribution "Knowledge-Aided (Potentially Cognitive) Transmit Signal and Receive Filter Design in Signal-Dependent Clutter". Dr. De Maio also is a Fellow member of IEEE.

Luca Pallotta (S'12, M'15, SM'18) received the Laurea Specialistica degree (cum laude) in telecommunication engineering in 2009 from the University of Sannio, Benevento, Italy, and the Ph.D. degree in electronic and telecommunication engineering in 2014 from the University of Naples Federico II, Naples, Italy. His research interest lies in the field of statistical signal processing, with emphasis on radar signal processing and radar targets classification. Dr. Pallotta won the Student Paper Competition at the IEEE Radar Conference 2013.